Photometric and spectroscopic investigation of nine Cepheids in the Cassiopeia constellation

J. Žák*[1,2], M. Skarka[1,2], E. Paunzen[1], P. Dubovský[3], M. Zejda[1] and G. Handler[4]

[1] *Department of Theoretical Physics and Astrophysics, Masaryk University, Kotlářská 2, CZ-611 37, Brno, The Czech Republic , (E-mail: 437396@mail.muni.cz)*

[2] *Astronomical Institute of the Czech Academy of Sciences 251 65 Ondřejov, The Czech Republic*

[3] *Vihorlat Astronomical Observatory, Mierová 4, SK-066 01 Humenné, The Slovak Republic*

[4] *Nicolaus Copernicus Astronomical Center, Bartycka 18, 00-716 Warsaw, Poland*

Abstract. We present new multicolor *BVRI* photometry and low-resolution spectroscopy of 9 fundamental mode Cepheids in the Cassiopeia constellation. Observations were carried out during the 2017/2018 observing season. We investigated each particular light curve in detail using Fourier decomposition techniques which we compare with the Cepheids from the OGLE project. Using the Gaia parallaxes and the period-luminosity relation we estimated the absolute magnitudes and constructed the Hertzsprung-Russell diagram. Our findings agree with the previously published results except for V824 Cas. This star has small Fourier amplitudes and shows a discrepancy in the absolute magnitudes based on Gaia and period-luminosity relation. We propose that V824 Cas can either be a member of a binary system or is not a fundamental-mode Cepheid but an overtone Cepheid.

Key words: Methods: Data Analysis – Techniques: Photometric – Techniques: Spectroscopic – Stars: Variables: Cepheids – Stars: Individual: V824 Cas

1. Introduction

Cepheids have played a prominent role in the history of astronomy. It was discovered that they change their brightness due to stellar pulsations (Shapley, 1914; Eddington, 1917). Leavitt & Pickering (1912) discovered the famous Period-Luminosity (P-L) relation, which ties the absolute magnitude with the pulsation period. This allows unprecedented distance measurements which makes Cepheids ideal objects for tracing the young population of the Milky Way Galaxy (Skowron et al., 2019; Benedict, McArthur, Feast, et al., 2007). Furthermore, classical Cepheids are the primary distance indicators for the extragalactic distance scale as they are used as standard candles. They provide a significant

contribution to the cosmic distance ladder as well as for the determination of the Hubble constant (Riess et al., 2018).

The typical Classical Cepheid is a young star with intermediate mass (3.5 to 15 $M_\odot$) which is a white-yellow population I supergiant (Catelan & Smith, 2015). Cepheids are radial pulsators which show periodic variations in radius, temperature, and brightness. The pulsation periods of Cepheids range from around 1 day to as long as 60 days. However, there are Cepheids observed in the Magellanic Clouds whose periods are longer than 100 days (Ulaczyk, Szymaski, Udalski, et al., 2013). The basic characterization of Cepheids can be performed by analysing their light curves. The shape of the light curves changes with the pulsation period. The amplitude of the light variations is wavelength dependent as it increases towards shorter wavelengths. Hertzsprung (1926) made the discovery that certain Cepheids show a relationship between the position of a bump on the light curve and the pulsation period. This phenomenon was named the "Hertzsprung progression".

Before the rapid growth of the automated surveys, such as OGLE (Udalski, Szymaski, Kaluzny, et al., 1992; Udalski, Szymański, & Szymański, 2015), ASAS-SN (Shappee, Prieto, Stanek, et al., 2014; Kochanek, Shappee, Stanek, et al., 2017) and many others, numerous observers (Szabados, 1981; Berdnikov, 2008) published multi-color observations of the Galactic Cepheids. These archival data have tremendous value as they can reveal evolutionary changes of the stars. The motivation of this work was to extend the time-base of multi-color observations for these stars.

The objective of this paper is to present new spectroscopic and $BVRI$ photometric data of nine fundamental mode Cepheids in the Cassiopeia constellation (sect. 2). The analysis and description of the light curves using Fourier decomposition technique are presented in Sect. 4.1. The comparison with the OGLE Galactic Bulge Cepheids is in Sect. 4.2. The astrophysical parameters of the targets are investigated in Sect. 5. The possible origin of the unusual behavior of V824 Cas is discussed in Sect. 6. The summary is given in Sect. 7.

2. Observations

Photometry of Galactic Cepheids in the Cassiopeia constellation was performed from fall 2017 to summer 2018 using the 600/2780 mm Newtonian telescope (equipped with G4-16000 Moravian Instruments Peltier cooled CCD camera with Johnsons-Cousins $BVRI$ filters) at Masaryk University Observatory (MUO), which is located in Brno, Czech Republic. The fundamental mode Cepheids were selected according to their location on the sky and their brightness to maximize the efficiency of the observations with the available equipment. The VSX catalog[1] (Watson, Henden, & Price, 2006) was used to eliminate Cepheids that were brighter than 10.3 magnitude in V-filter light maximum to ensure that the star

---

[1] https://www.aavso.org/vsx/

would not saturate with exposure times below 10 seconds. On the other hand, we omitted stars fainter than 11.8 mag in their V-filter light minimum to avoid exposure times above 90 s in B and to ensure a good signal to noise ratio. At last, we tried to select only stars that are apparently not blended. The selected stars together with the observing log are listed in Table 1. The photometric data are avaiable at
http://www.astro.sk/caosp/Eedition/FullTexts/vol49no3/pp503-521.dat/.

Table 1. Details to the investigated stars (taken from the VSX database). Cepheids are arranged according to increasing value of the pulsation period. The observation log presents the number of nights per star (#N) and the average number of frames per star in each of the filters (#f). The symbols in the last column are used in the forthcoming figures.

Star name	Sp. type	V [mag]	$(B\text{-}V)$ [mag]	#N	#f	
DF Cas	F6-G4	10.53 - 11.13	1.372	12	160	●
V395 Cas	G3	10.39 - 10.95	0.827	10	129	■
UZ Cas	F6-G2	10.93 - 11.73	1.082	13	127	▲
CG Cas	F5-F8	10.89 - 11.73	1.228	15	123	▼
CF Cas	F8Ib-G0Ib	10.80 - 11.47	1.156	15	136	◆
DW Cas	F7	10.81 - 11.41	1.288	8	82	▶
V824 Cas		11.03 - 11.36	1.272	11	89	◀
BP Cas	F6-G1	10.55 - 11.33	1.537	11	115	★
CH Cas	F3pIb-F6	10.47 - 11.56	1.755	13	57	⬟

Altogether, 4069 frames were obtained during 25 nights. All obtained frames were corrected for dark count and flat field using CMUNIPACK (Motl, 2011). Aperture photometry was also performed in CMUNIPACK. The star field containing CF Cas and CG Cas also contained a star cluster NGC 7790, which has been used for calibration to the standard system (Henden, 1999).

The spectroscopic observations (October and November 2018) were taken at the Astronomické observatórium na Kolonickom sedle (Slovak Republic) with a Schmidt-Cassegrain Celestron C11 telescope: aperture diameter 280 mm and an effective focal length of 1750 mm. The used LISA spectrograph (Shelyak) covers a wavelength region from 3 800 to 7 500 Å with a resolving power of about 1 000. The signal-to-noise ratios are between 50 and 100. The spectra are shown in Fig. 1.
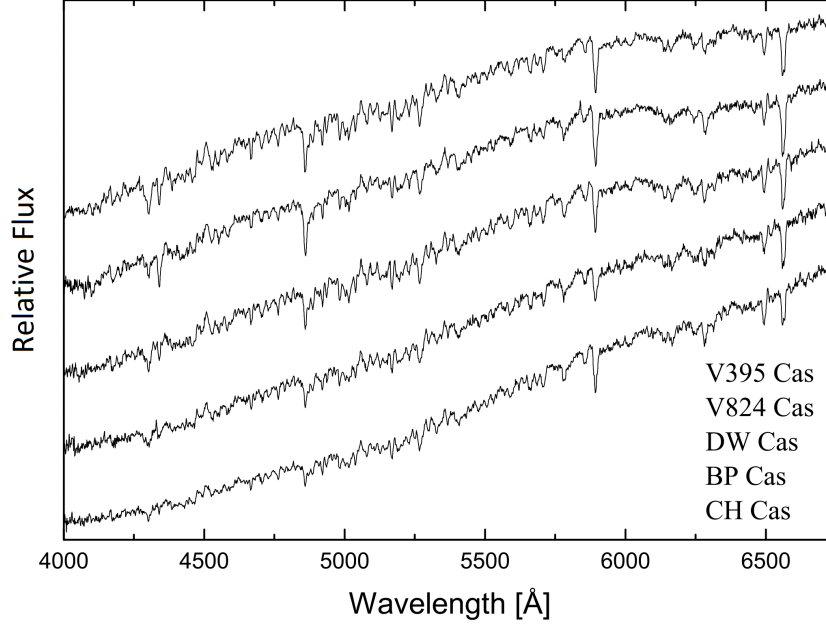
Figure 1. Classification resolution spectra of V824 Cas and four other investigated Cepheids of comparable spectral types.

3. Methods and analysis

3.1. New period determination

We have recalculated periods for all of the stars in our sample using ASAS-SN data. The PERSEA software (Maciejewski, 2007, based on the algorithm by Schwarzenberg-Czerny (1996)) was used to determine new periods. These calculations for each star were based on over 500 data points in a time range of approximately 1000 days. The periods can be found in Table 2. We show an example of the phase curves before and after recalculation of the period in Fig. 2 for V824 Cas. Note that the former period was based on data spanning only 13 days with typically 2 points per night.

3.2. Light curve fitting and Fourier coefficients

For the investigation of the light curves, we performed a fit with sine series

$$m(t) = A_0 + \sum_{i=1}^{N} a_i \, \cos(i\omega(t - t_0)) + \sum_{i=1}^{N} b_i \, \sin(i\omega(t - t_0)), \tag{1}$$

Table 2. The periods of the sample stars. The second column shows the periods given in VSX. Newly calculated periods with the errors are given in the third column of the table.

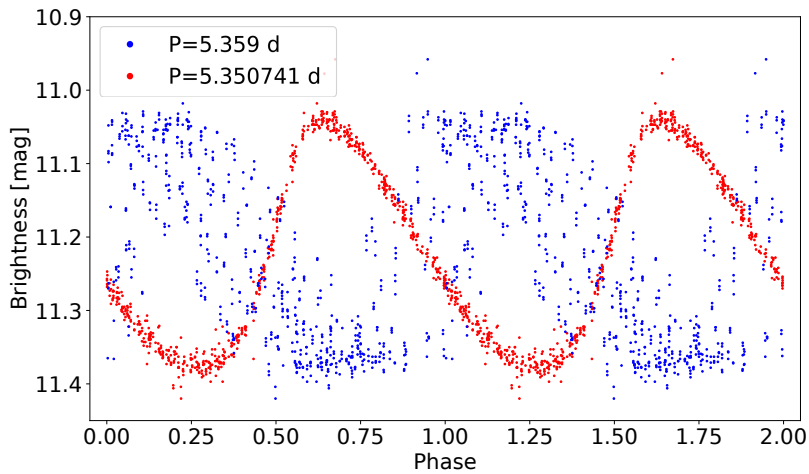| Star name	Period in literature [d]	Calculated period [d]
DF Cas	3.832472	3.8324(5)
V395 Cas	4.037728	4.0380(5)
UZ Cas	4.259459	4.2595(6)
CG Cas	4.36554	4.3653(6)
CF Cas	4.87522	4.8750(7)
DW Cas	4.99776	4.9978(8)
V824 Cas	5.359	5.3507(9)
BP Cas	6.272724	6.272(1)
CH Cas	15.09215	15.098(7)

Figure 2. The comparison of the ASAS-SN data phased with former and newly determined period for V824 Cas.

where $m(t)$ is the observed magnitude at time t, A_0 is the mean magnitude, a_i, b_i are the amplitude components of the i-th harmonic, $\omega = 2\pi/P$ is the angular frequency, P is the period, N is the order of the series and t_0 is the epoch of maximum light.

The eq. 1 can also be written in the following more compact form that we

used in our analysis:

$$m(t) = A_0 + \sum_{k=1}^{N} A_k \ \sin(2\pi k \frac{(t-t_0)}{P} + \phi_k), \qquad (2)$$

For all studied stars, we used a Fourier fit of the fourth order since it performed well in the visual test. Period P is presented at the bottom of each graph in Fig. 3.
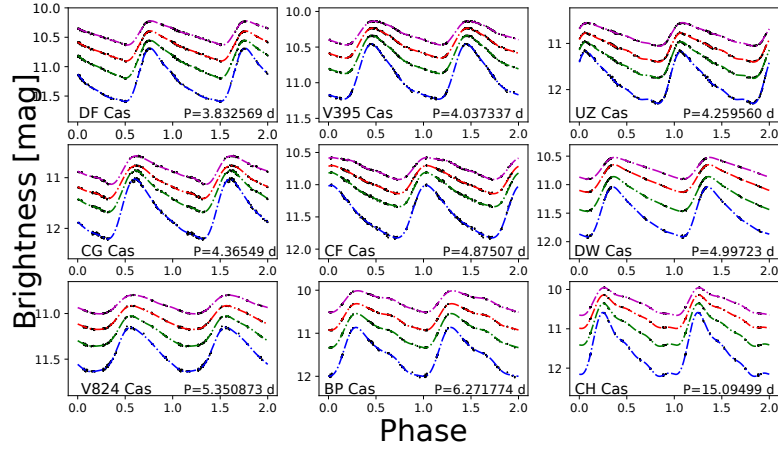

Figure 3. The phase curves of all studied stars. The phase curves are vertically shifted for a better visibility. Blue, green, red and magenta colors mark B, V, R and I filters respectively.

The light curves of well-observed Cepheids can be described by using Fourier coefficients, which were introduced by Schaltenbrand & Tammann (1971) and further developed by Simon & Lee (1981), who used it for studying structural properties of Cepheid light curves. These coefficients are defined as

$$R_{i1} = \frac{A_i}{A_1}; \ \phi_{i1} = \phi_i - i\phi_1, \qquad (3)$$

where amplitudes of the sine series are denoted with A and phases with ϕ. The index i is larger than 1.

4. Results

4.1. Amplitudes and Fourier Coefficients

We have used the ASAS-SN data (Shappee, Prieto, Stanek, et al., 2014; Kochanek, Shappee, Stanek, et al., 2017), and the Nitro database (Morgan, 2003) to compare our results with the other sources. The Nitro database contains data and Fourier coefficients for more than 1000 Galactic variables of which many are Cepheids. Except for V824 Cas[2], all studied stars are listed in this database. Data are in the V filter and are from different sources for all the stars. The data sources are listed in Table 3.

Table 3. The data sources for the Fourier coefficients in V filter.

Star	Source of data
DF Cas	Antonello, Poretti, & Reduzzi (1990)
UZ Cas	Antonello, Poretti, & Reduzzi (1990)
CG Cas	Antonello, Poretti, & Reduzzi (1990)
CF Cas	Moffett & Barnes (1985)
BP Cas	Simon & Lee (1981)
CH Cas	Antonello & Morelli (1996)
V824 Cas	Berdnikov (2008)

The comparison shows a good agreement for the majority of the stars (Fig. 4). One of the common reasons for the data discrepancy of the compared coefficients is the sparse coverage of the phase curves of data acquired at MUO. This is most noticeably apparent for CG Cas, DW Cas, and CH Cas (see the corresponding panels in Fig. 3). The discrepancy could also be caused by the different order of the Fourier fit and by the quality of the data from the literature. The data obtained at MUO are fitted with a Fourier fit of the fourth order. On the other hand, the order of the fit from the Nitro database varies from the third to the seventh order. Another cause can originate from various time bases of acquired data sets. The MUO data were obtained during roughly 10 months, ASAS-SN data were obtained during more than 30 months. These effects combined together preclude from obtaining results within the errorbar range.

From Fig. 3 it is apparent that the amplitude of the light curve is clearly wavelength dependent as it increases towards shorter wavelengths. Fig. 5 shows the pulsation amplitude of Cepheids in our sample in various passbands as a function of the pulsation period. Amplitudes and Fourier coefficients in all filters are listed in Tables 5-8 in the Appendix. V824 Cas exhibits unexpectedly low values of the amplitude for all filters when compared to the observations and the theoretical predictions shown in Bhardwaj, Kanbur, Marconi, et al. (2017).

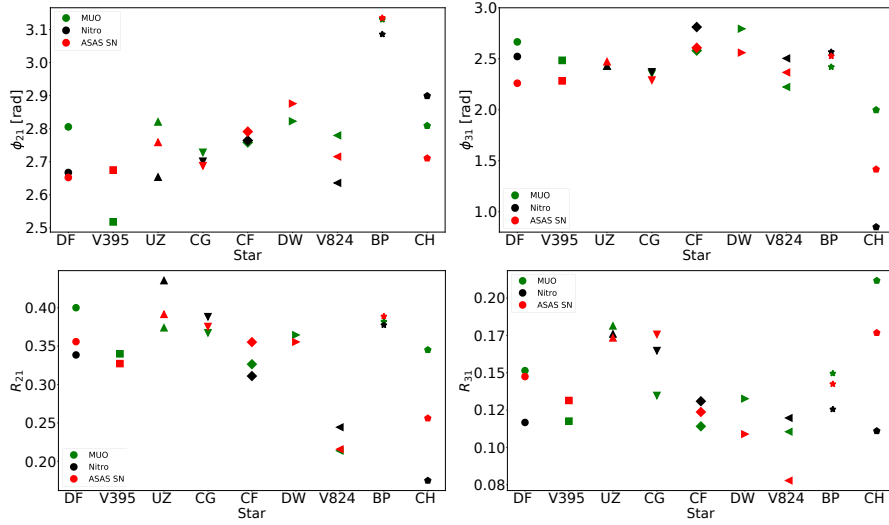
[2]Data taken from Berdnikov (2008).

Figure 4. The comparison of Fourier coefficients to ASAS-SN data and to literature data. The symbols for the stars are the same as in Table. 1.
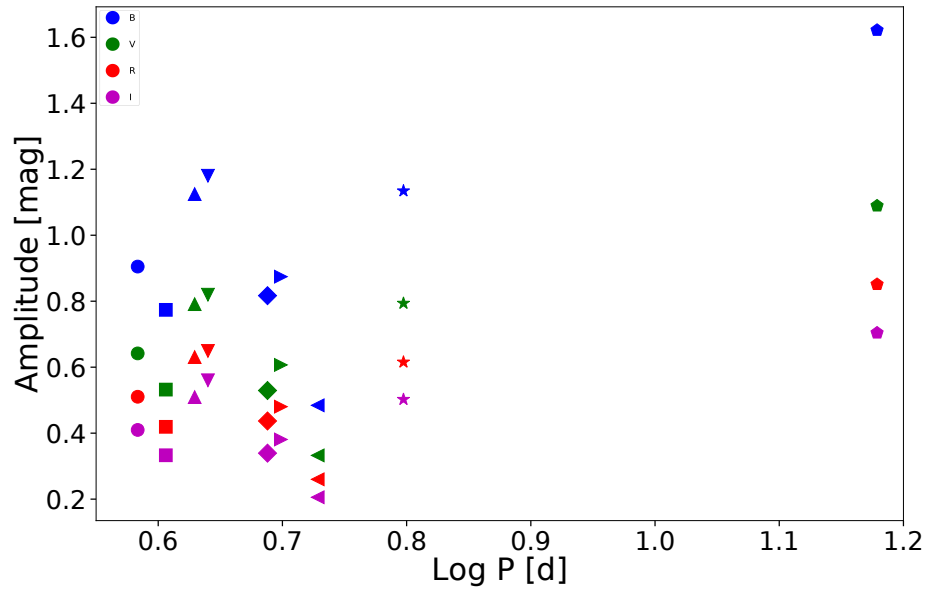

Figure 5. The light-curve amplitude dependency on the logarithm of the period for all filters. The symbols of the stars are defined in the last column of Table 1.

The Fourier parameters as a function of the pulsation period are shown in Fig. 6. The amplitude dependency on the wavelength results in clear dependency and systematics of ϕ_{21} and ϕ_{31} in different filters. However, the amplitude coefficients R_{21} and R_{31} lack this dependency (see Fig. 6).
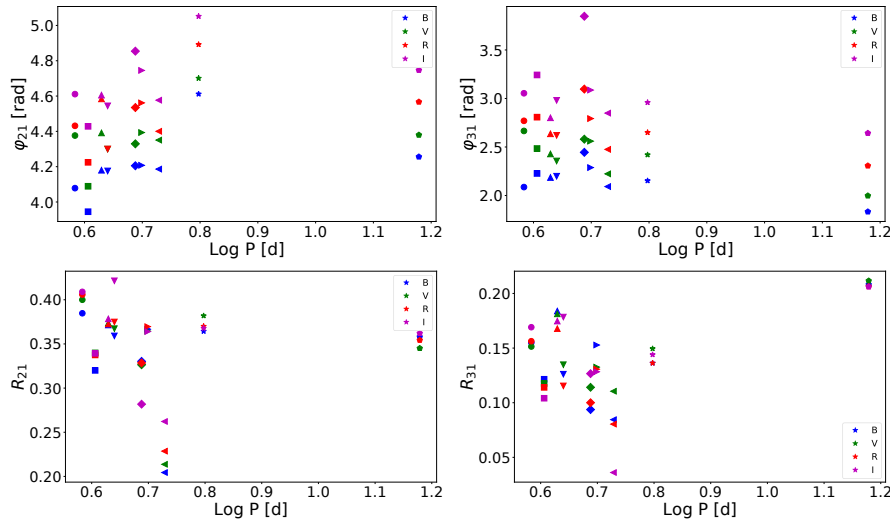

Figure 6. The obtained Fourier coefficients in different filters. The symbols of the stars are defined in the last column of Table 1

The period dependencies of obtained coefficients shown in Fig. 6 are in good agreement with the progressions predicted theoretically by Bhardwaj, Kanbur, Marconi, et al. (2017). The coefficient ϕ_{21} shows a clear rise with an increasing period from $\log(P) \sim 0.6$ d to $\log(P) \sim 0.8$ d. In Fig. 6, it can be seen that the coefficient ϕ_{31} is at the expected plateau which lasts from $\log(P) \sim 0.6$ d to $\log(P) \sim 0.8$ d.

The value of the R_{21} is not changing much. An exception is V824 Cas which shows significantly lower values of this coefficient (Fig. 6). Parameter R_{31} is slightly decreasing with increasing period until $\log(P) \sim 0.8$ d. Again, V824 Cas shows unexpectedly low values.

4.2. Comparison to OGLE data

The Optical Gravitational Lensing Experiment (OGLE, Udalski, Szymaski, Kaluzny, et al., 1992; Udalski, Szymański, & Szymański, 2015) is a survey with the main objective of searching for the dark matter with microlensing phenomena. As a byproduct, it has discovered several exoplanets (Bond et al., 2004) and created an enormous database of variable stars data. The main targets of in-

terest are specifically the Magellanic Clouds and the Galactic Bulge. Soszyński, Udalski, Szymaski, et al. (2015, 2017) have published an analysis of OGLE data and calculated Fourier coefficients for Cepheids in the Large and Small Magellanic Clouds (LMC and SMC) and the Galactic Bulge. We compare the Fourier coefficients in I filter from MUO and OGLE, because OGLE observations are made mostly in I filter[3]. The same markers for each star were used as originally in Table 1 are used in Fig. 7.
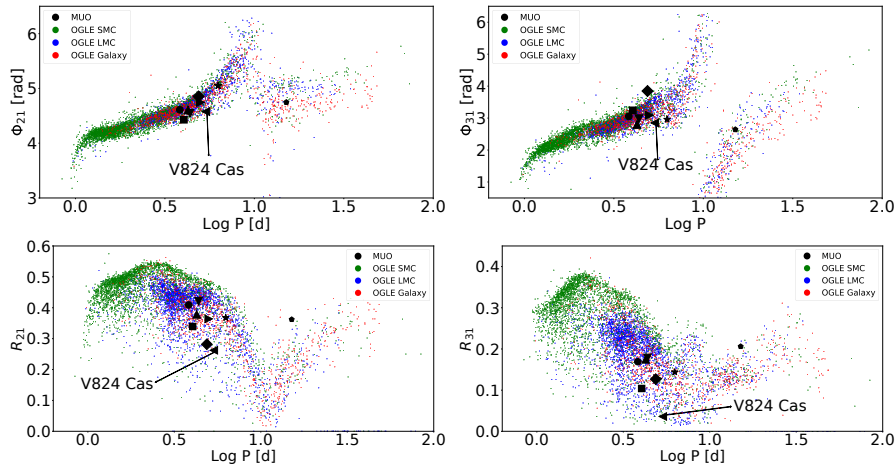

Figure 7. The comparison of the Fourier coefficients to OGLE Cepheids in the SMC, LMC and Galactic Bulge. The symbols for the stars are the same as in Tab. 1.

We can see a good agreement for most of the stars (Fig. 7). V824 Cas shows the largest deviation from the trends. The cause of the deviation towards lower values can have many origins: from data uncertainty to the physical origin. Literature data in Fig. 4 show even lower values than data obtained at MUO for ϕ_{21} and R_{31}. This may be an indication that the data are correct and V824 Cas could be a peculiar Cepheid.

Another star that differs from the general trends is CF Cas which has higher values of ϕ_{31} and lower values of R_{21} (Fig. 7). Coefficients from the literature (section 4.1) show a good agreement with the ones obtained at MUO, thus, we can conclude that the higher values are of a physical origin and not rather caused by the data uncertainty.

A very interesting is the comparison of R_{31} coefficient in Fig. 7 as there is a clear separation of Cepheids located in LMC, SMC, and Bulge. The value of the R_{31} coefficient decreases as the metallicity increases (Bhardwaj, Kanbur, Marconi, et al., 2017). The difference is because LMC, SMC and Galactic Bulge

---

[3]The coefficients were obtained from ftp://ftp.astrouw.edu.pl/ogle4/OCVS/

have different metallicity. The data from MUO nicely fits in this sequence when solar metallicity $Z = 0.02$ is used. $Z_{\mathrm{SMC}} = 0.004$ and $Z_{\mathrm{LMC}} = 0.008$ (Glatt, Grebel, & Koch, 2010). Stars located in the Galactic Bulge span metallicity range $-1.5 \lesssim [\mathrm{Fe/H}] \lesssim 0.5$ (Barbuy, Chiappini, & Gerhard, 2018). This explains the widespread of values for OGLE Bulge Cepheids in the diagram.

5. Physical parameters

It is well known that Cepheids show a relatively wide range of effective temperatures (up to $1500\,\mathrm{K}$) and thus colors during their pulsational phases (Fernley, Skillen, & Jameson, 1989). Therefore, we use here mean colors for all objects. The reddening values and metallicities were taken from the paper by Groenewegen (2018) whereas the mean $(B - V)$ and V values were taken from the catalog by Fernie, Beattie, Evans, et al. (1995). Only one star, V824 Cas, is not included in these references. For this object, the BV magnitudes were taken from Kharchenko (2001). This all-sky catalogue of more than 2.5 million stars transformed the Hipparcos/Tycho BV magnitudes in standard Johnson ones, using a homogenized transformation law. The reddening value was interpolated within the corresponding maps published by Green, Schlafly, Finkbeiner, et al. (2018) using the range of distances from the Gaia DR2 (Bailer-Jones et al., 2018). We also compared the published reddening values of the other targets from Groenewegen (2018) with the reddening map which yields an excellent agreement.

To estimate the absolute magnitudes of our targets, we used the PLZ relation from Groenewegen (2018) and the basic approach applying the parallaxes from the Gaia DR2 (Lindegren, Hernández, Bombrun, et al., 2018). We compared the absolute magnitudes from three different PLZ relations using V, K, and the reddening-free Wesenheit index. The results of all three relations are in excellent agreement from which we conclude that the photometry is consistent and that the reddening values are correct. The errors of the absolute magnitudes were calculated with a full propagation of uncertainties, i.e. the parallax errors and the V amplitudes as listed in Table 6.

We checked, if the metallicities of our targets deviate significantly from the solar. In a series of papers, Andrievsky, Luck, Korotin (2014) published detailed abundances of Cepheids. All but V824 Cas are included in these papers. Two stars, CH Cas and DF Cas, are slightly overabundant (about $0.2\,\mathrm{dex}$) in [Fe/H]. Using these metallicities and using the corresponding PLZ relation from Groenewegen (2018), the difference to the absolute magnitude from the PLZ relation is only $0.04\,\mathrm{mag}$, respectively. This is negligible compared to the other error sources.

The parallaxes, colors, reddening values, and absolute magnitudes together with their errors are listed in Tab. 4. The comparison of the absolute magnitudes shows that only V824 Cas is outstanding with non-compatible values. This fits

Table 4. Parallaxes, colors, reddening values, and absolute magnitudes for our our targets. The latter were derived from the parallaxes (M_V^{Gaia}) and the PL relation (M_V^{PL}) taken from Groenewegen (2018).

Star name	Parallax [mas]	$(B - V)$ [mag]	$E(B - V)$ [mag]	M_V^{Gaia} [mag]	M_V^{PL} [mag]
DF Cas	0.307(28)	1.181	0.564(499)	-3.45(38)	-3.31(20)
V395 Cas	0.247(68)	1.146	0.565(56)	-4.05(65)	-3.37(20)
UZ Cas	0.149(30)	1.110	0.469(34)	-4.22(59)	-3.42(21)
CG Cas	0.224(30)	1.250	0.667(9)	-3.95(50)	-3.45(21)
CF Cas	0.287(32)	1.174	0.556(21)	-3.28(36)	-3.56(21)
DW Cas	0.355(26)	1.475	0.807(32)	-3.62(35)	-3.59(22)
V824 Cas	0.206(28)	1.272	0.810(50)	-4.87(34)	-3.66(22)
BP Cas	0.374(28)	1.550	0.864(14)	-3.86(43)	-3.82(23)
CH Cas	0.271(28)	1.650	0.942(36)	-4.73(59)	-4.73(28)

very well in the peculiar light curve parameters (see Sect. 4.1). This star is discussed in Sect. 6.

As the last step, we located our targets in $(B - V)_0$ versus M_V diagram in order to check if they populate the known Cepheid domain. In Fig. 8 the results are plotted together with the solar-abundance ([Z] = 0.019) isochrones taken from the PARSEC database (Bressan, Marigo, Girardi, et al., 2012).

It is well known that a star may cross the Cepheid instability strip on the Hertzsprung-Russell (HR) diagram more than once during its evolution. After the exhaustion of hydrogen in the core, it expands to become a red giant and then crosses the instability strip rapidly on a Kelvin-Helmholtz time scale. It climbs the red giant branch to the red giant tip and after the ignition of helium burning in the core (a relatively long-lived evolutionary stage) it may make a loop to a higher temperature in the HR diagram. As can be seen from Fig. 8 our targets may cover these two different evolutionary stages with ages between 40 and 100 Myr, respectively. Again, V824 Cas is outstanding because it is brighter than normal Cepheids for the given color and period. We note that the pulsation phase at which the input values were taken for V824 Cas is unknown, thus, possibly introducing further uncertainty in HRD position.

6. Origin of the peculiar behavior of V824 Cas

It is seen in Fig. 5 that V824 Cas exhibits unexpectedly low amplitudes in all photometric bands. The unusually low amplitudes of V824 Cas brings up the question of whether the Cepheid is correctly classified.

A special class of Cepheids, the so-called s-Cepheids (sometimes called DCEPS), are delta Cephei variables with photometric amplitude below 0.5 mag in V (0.7 mag in B) and almost symmetrical light curves, their period is usually shorter than $P < 7$ d (Samus' et al., 2017). Most likely they are first-overtone pulsators. First overtone Cepheids follow different P-L relation than the funda-
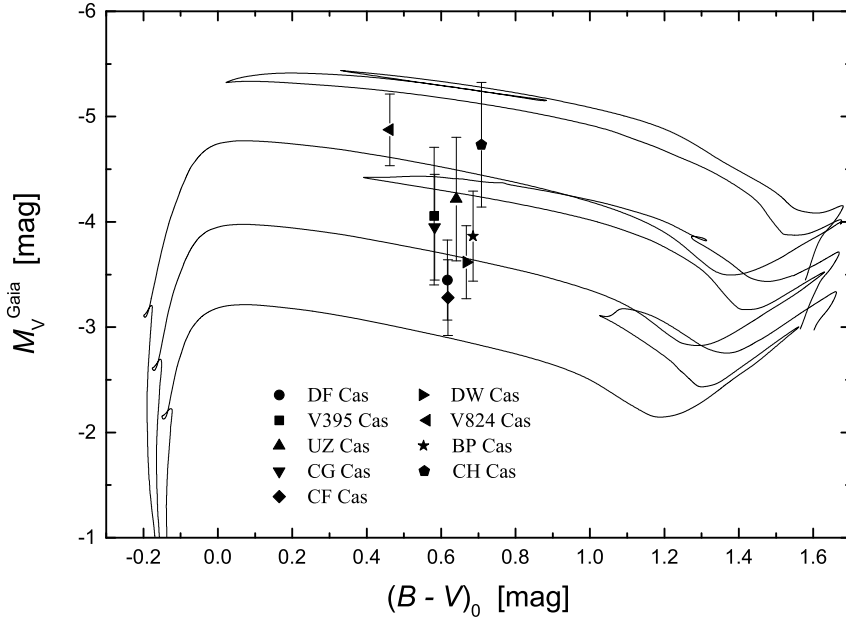
Figure 8. The (B - V)₀ versus M_V diagram of our program stars together with the solar-abundance ([Z] = 0.019) isochrones (log t = 8.0, 7.8, and 7.6) taken from the PARSEC database (Bressan, Marigo, Girardi, et al., 2012).

mental ones (Udalski et al., 1999) as they are brighter for a given period. As can be seen in the Fig. 8 V824 Cas has high luminosity which is suggesting overtone nature.

The methodology described in a paper by Antonello, Poretti, & Reduzzi (1990) gives two suitable criteria to distinguish the s-Cepheids from their normal amplitude relatives using the Fourier parameters. S-Cepheids should form a lower sequence below the normal amplitude Cepheids sequence in the R_{21} versus pulsation period plot. Another criterion was postulated as the s-Cepheids should form an upper sequence above the normal amplitude Cepheids in the ϕ_{31} versus period plot.

It can be seen that the first criterion is met, however, the second has failed (Fig. 6). Thus, the classification of V824 Cas as s-Cepheid is not conclusive. Turner, Usenko, & Kovtyukh (2006) have shown that a sinusoidal light curve is not a conclusive evidence for overtone pulsations and that high-resolution spectroscopic observations are needed to determine the pulsation mode.

Another explanation for the unusual amplitude can be a binary status. Binarity plays a relevant role when investigating the observed amplitudes of Cepheids, as more than 50 % of the Galactic Cepheids belong to binary or mul-

tiple systems (Szabados, 2003). The presence of a companion can affect the photometric amplitudes and cause a reduction of the observable amplitude of the brightness variation due to the presence of a constant source of light. This was used in a paper by Coulson & Caldwell (1989) on the sample of Cepheids to hint a possibility of a hidden companion for Cepheids that deviate from a constant trend.

We have investigated the RUWE [4] coefficient ϱ computed in Gaia DR2 (Gaia Collaboration et al., 2018; Lindegren, Hernández, Bombrun, et al., 2018). Values above $\varrho > 1.4$ can hint a possible binarity. However, all Cepheids in our sample have values between 0.85 and 1.07. A known spectroscopic binary Cepheid in our sample CG Cas (Szabados, 1996) has a value of $\varrho = 0.981$. Also, we have compared the Gaia DR2 parallax errors in Table 4 to check for any deviations. Only V395 Cas has double the parallax error compared to the other stars, also possibly hinting a companion presence.

As shown by Tanvir (1997) the amplitude ratio A_I/A_V is not dependent on the period and has a constant value of $A_I/A_V \sim 0.64$. V824 Cas exhibits deviation from this value, which might imply the presence of a companion. This finding deserves further, more complex, both photometric and spectroscopic investigations as there are no spectroscopic measurements available in the literature. It is worth to mention that the Gaia DR2 catalog data do not suggest the presence of a visual companion that could affect the amplitude.

Unusually high metallicity of V824 Cas might be another explanation of its unexpected behavior. The amplitude coefficient R_{31} is metallicity dependent so that with an increasing metallicity the value of R_{31} decreases (Fig. 7). Since no abundance estimates for V824 Cas are available in the literature, we compared our classification resolution spectra of all targets in order to search for any significant enhancements. In Fig. 1, five spectra are plotted. The metallic line spectrum of V824 Cas is comparable to those of the other four targets. We can, therefore, rule out this scenario.

7. Summary and conclusions

We present an analysis of DF Cas, V395 Cas, UZ Cas, CG Cas, CF Cas, DW Cas, V824 Cas, BP Cas and CH Cas based on new $BVRI$ photometry and low-resolution spectroscopy. The observations were carried out during 25 nights in 2017/2018 using 600-mm telescope at Masaryk University Observatory, Brno, Czech Republic (photometry) and Astronomické observatórium na Kolonickom sedle, Slovak Republic (spectroscopy).

We have performed new period determinations for all the stars in our sample as previous data were obsolete or not precise enough. The photometric data were fitted with a Fourier fit of the fourth-order to obtain the Fourier coefficients. By

---

[4]https://www.cosmos.esa.int/web/gaia/dr2-known-issues

comparing our results with those from the literature we find no major deviations except for V824 Cas which shows unusually low amplitudes.

Employing the Gaia DR2 parallaxes and available photometric measurements and reddening maps we estimated the absolute magnitudes of the sample Cepheids and constructed an HR diagram. We found that all the targets are located within the classical Cepheid instability strip with ages between 40 and 100 Myr. Except for V824 Cas, the absolute magnitudes based on the parallaxes and the *PL* relations are in agreement within the error bars. This behavior also points towards a peculiarity of V824 Cas.

V824 Cas appears to have an extraordinary low pulsation amplitude and amplitude Fourier coefficients compared to other Cepheids. From a comparison with literature data and parameters based on the ASAS-SN photometry, we can exclude an instrumental origin of the peculiarity. We propose two possible explanations of the peculiar behavior. V824 Cas could either be an s-Cepheid (DCEPS) or a classical Cepheid in a binary system. We recommend to obtain a high-resolution spectroscopic data to solve the status of V824 Cas.

References

Andrievsky S. M., Luck R. E., Korotin S. A.: 2014, *Mon. Not. R. Astron. Soc.* **437**, 2106

Antonello E., Morelli P. L.: 1996, *Astron. Astrophys.* **314**, 541

Antonello E., Poretti E., Reduzzi L.: 1990, *Astron. Astrophys.* **236**, 138

Bailer-Jones C. A. L., Rybizki J., Fouesneau M., Mantelet G., Andrae R.: 2018, *Astron. J.* **156**, 58

Barbuy, B., Chiappini, C., & Gerhard, O. 2018, *Ann. Rev. Astron. Astrophys.* **56**, 223

Benedict G. F., McArthur B. E., Feast M. W., et al.: 2007, *Astron. J.* **133**, 1810

Berdnikov, L. N.: 2008, *VizieR Online Data Catalog* **2285**

Bhardwaj A., Kanbur S. M., Marconi M., et al.: 2017, *Mon. Not. R. Astron. Soc.* **466**, 2805

Bond, I. A., Udalski, A., Jaroszyński, M., et al.: 2004, *Astrophys. J., Lett.* **606**, L155

Bressan A., Marigo P., Girardi L., et al.: 2012, *Mon. Not. R. Astron. Soc.* **427**, 127

Catelan M., Smith H. A., 2015, *Pulsating stars*, Wiley-VCH, United States

Coulson I. M., Caldwell J. A. R.: 1989, *Mon. Not. R. Astron. Soc.* **240**, 285

Eddington A. S.: 1917, *Observatory* **40**, 290

Fernie J. D., Beattie B., Evans N. R., Seager S.: 1995, *Inf. Bull. Variable Stars* **4148**, 1

Fernley J. A., Skillen I., Jameson, R. F.: 1989, *Mon. Not. R. Astron. Soc.* **237**, 947

Gaia Collaboration, Brown, A. G. A., Vallenari, A., et al.: 2018, *Astron. Astrophys.* **616**, A1

Glatt K., Grebel E. K., Koch A.: 2010, *Astron. Astrophys.* **517**, A50

Green G. M., Schlafly E. F. Finkbeiner D.: 2018, *Mon. Not. R. Astron. Soc.* **478**, 651

Groenewegen M. A. T.: 20018, *Astron. Astrophys.* **619**, A8

Henden A.: 1999, *online*
  http://binaries.boulder.swri.edu/fields/ngc7790.html

Hertzsprung E.: 1926, *Bull. Astron. Inst. Netherlands* **3**, 115

Kharchenko N. V.: 2001, *Kinematika i Fizika Nebesnykh Tel* **17**, 409

Kochanek C. S., Shappee B. J., Stanek K. Z., et al.: 2017, *Publ. Astron. Soc. Pac.* **129**, 104502

Leavitt H. S., Pickering E. C., et al.: 1912, *Harvard Circ.* **173**, 1

Lindegren L., Hernández J., Bombrun A., et al.: 2018, *Astron. Astrophys.* **616**, A2

Maciejewski G.: 2007, *online* PᴇʀSᴇᴀ,
  http://www.astri.uni.torun.pl/

Moffett T. J., Barnes T. G., III, et al.: 1985, *Astrophys. J., Suppl.* **58**, 843

Morgan S.: 2003, *online* Nitro database,
  http://nitro9.earth.uni.edu/

Motl D.: 2011, *online* CMᴜɴɪPᴀᴄᴋ,
  http://c-munipack.sourceforge.net/

Riess, A. G., Casertano, S., Yuan, W., et al.: 2018, *Astrophys. J.* **861**, 12

Samus' N. N., Kazarovets E. V., Durlevich O. V., Kireeva N. N., Pastukhova E. N.: 2017, *Astronomy Reports* **61**, 80

Schaltenbrand R., Tammann G.: 1971, *Astron. Astrophys., Suppl. Ser.* **4**, 265

Schwarzenberg-Czerny A.: 1996, *Astrophys. J.* **460**, L107

Shapley H.: 1914, *Astrophys. J.* **40**, 448

Shappee B., Prieto J., Stanek K.Z., et al.: 2014, *American Astronomical Society* **223**, 236.03

Simon N. R., Lee A. S.: 1981, *Astrophys. J.* **248**, 291

Skowron, D. M., Skowron, J., Mróz, P., et al.: 2019, *Science* **365**, 478

Soszyski I., Udalski A., Szymaski M.K., et al.: 2015, *Acta Astron.* **65**, 297

Soszyski I., Udalski A., Szymaski M.K., et al.: 2017, *Acta Astron.* **67**, 297

Szabados, L.: 1981, *Commmunications of the Konkoly Observatory* **77**, 1

Szabados L.: 1996, *Astron. Astrophys.* **311**, 189

Szabados L.: 2003, *Inf. Bull. Variable Stars* **5394**, 1

Tanvir N. R.: 1997, *EDS proceedings* **91**

Turner D. G., Usenko I. A., Kovtyukh V. V.,: 2006, *Observatory* **126**, 207

Udalski A., Szymaski M., Kaluzny J., et al.: 1992, *Acta Astron.* **42**, 253

Udalski, A., Szymanski, M., Kubiak, M., et al.: 1999, *Acta Astron.* **49**, 201

Udalski A., Szymański M. K., Szymański G.: 2015, *Acta Astron.* **65**, 1

Ulaczyk K., Szymaski M. K., Udalski A., et al.: 2013, *Acta Astron.* **63**, 159

Watson C. L., Henden A. A., Price A.: 2006, *Society for Astronomical Sciences Annual Symposium* **25**, 47

A. Appendix

Table 5. Amplitude and Fourier coefficients of the sample Cepheids in B filter. Values in the parenthesis are obtained errors.

Star	A [mag]	A_0 [mag]	A_1 [mag]	R_{21}	R_{31}	R_{41}	Φ_1 [rad]	Φ_{21} [rad]	Φ_{31} [rad]	Φ_{41} [rad]
DF Cas	0.91	12.133(1)	0.386(2)	0.385(4)	0.155(5)	0.075(6)	0.842(4)	2.508(17)	5.228(30)	1.643(63)
V395 Cas	0.77	11.918(1)	0.352(2)	0.320(4)	0.121(4)	0.036(4)	3.609(4)	2.374(18)	5.369(43)	1.43(14)
UZ Cas	1.13	12.488(3)	0.474(4)	0.371(7)	0.184(10)	0.104(7)	2.276(7)	2.609(29)	5.327(42)	2.074(73)
CG Cas	1.18	12.605(4)	0.514(3)	0.359(7)	0.126(7)	0.037(5)	1.025(14)	2.605(42)	5.340(75)	2.48(23)
CF Cas	0.82	12.369(1)	0.365(2)	0.330(6)	0.094(5)	0.303(5)	2.212(5)	2.634(16)	5.587(56)	2.02(17)
DW Cas	0.87	12.647(1)	0.375(4)	0.367(13)	0.150(13)	0.056(11)	1.173(11)	2.637(37)	5.429(70)	1.99(17)
V824 Cas	0.48	12.475(2)	0.235(2)	0.204(8)	0.085(13)	0.043(11)	4.798(8)	2.615(54)	5.234(89)	1.89(21)
BP Cas	1.13	12.502(2)	0.491(4)	0.364(6)	0.136(6)	0.051(10)	1.840(5)	3.041(23)	5.294(47)	2.53(10)
CH Cas	1.62	12.752(5)	0.671(7)	0.358(18)	0.208(9)	0.133(12)	0.328(14)	2.625(34)	4.98(10)	1.38(12)

Table 6. Amplitude and Fourier coefficients for the sample Cepheids in V filter.

Star	A [mag]	A_0 [mag]	A_1 [mag]	R_{21}	R_{31}	R_{41}	Φ_1 [rad]	Φ_{21} [rad]	Φ_{31} [rad]	Φ_{41} [rad]
DF Cas	0.64	10.906(1)	0.265(1)	0.400(4)	0.151(5)	0.067(6)	0.712(5)	2.805(17)	5.807(33)	2.340(65)
V395 Cas	0.53	10.644(1)	0.237(1)	0.340(4)	0.118(4)	0.042(4)	3.509(5)	2.518(19)	5.626(46)	1.91(13)
UZ Cas	0.79	11.415(2)	0.330(3)	0.374(8)	0.181(10)	0.108(8)	2.184(7)	2.820(33)	5.570(47)	2.312(77)
CG Cas	0.82	11.317(3)	0.349(2)	0.367(7)	0.135(7)	0.022(6)	0.961(14)	2.729(41)	5.498(70)	3.01(38)
CF Cas	0.53	11.104(1)	0.237(1)	0.326(6)	0.114(6)	0.056(5)	2.120(5)	2.759(18)	5.722(49)	2.349(98)
DW Cas	0.61	11.197(1)	0.259(2)	0.364(10)	0.133(8)	0.041(8)	1.083(7)	2.823(24)	5.702(64)	1.99(18)
V824 Cas	0.33	11.213(1)	0.159(1)	0.214(6)	0.111(9)	0.041(7)	4.742(6)	2.780(37)	5.365(57)	1.65(19)
BP Cas	0.79	10.970(1)	0.335(2)	0.382(5)	0.150(4)	0.049(8)	1.293(4)	3.130(16)	5.561(32)	3.135(71)
CH Cas	1.09	11.019(3)	0.454(5)	0.345(17)	0.212(6)	0.138(11)	0.226(13)	2.809(31)	5.139(95)	1.712(98)

Table 7. Amplitude and Fourier coefficients of the sample Cepheids in R filter.

Star	A [mag]	A_0 [mag]	A_1 [mag]	R_{21}	R_{31}	R_{41}	Φ_1 [rad]	Φ_{21} [rad]	Φ_{31} [rad]	Φ_{41} [rad]
DF Cas	0.51	10.469(1)	0.209(1)	0.406(6)	0.156(7)	0.068(8)	0.650(7)	2.861(22)	5.911(44)	2.510(87)
V395 Cas	0.42	10.064(1)	0.186(1)	0.338(5)	0.114(5)	0.046(5)	3.431(6)	2.664(23)	5.949(58)	2.29(14)
UZ Cas	0.63	10.814(2)	0.264(3)	0.373(9)	0.168(11)	0.119(8)	2.100(8)	3.013(35)	5.778(56)	2.666(79)
CG Cas	0.65	10.807(3)	0.275(2)	0.375(8)	0.115(8)	0.045(8)	0.943(16)	2.729(45)	5.761(90)	3.76(17)
CF Cas	0.44	10.628(1)	0.193(1)	0.328(7)	0.100(7)	0.034(6)	2.031(6)	2.964(21)	6.238(67)	2.59(18)
DW Cas	0.48	10.407(1)	0.203(2)	0.37(11)	0.131(9)	0.044(8)	0.991(8)	2.990(26)	5.935(73)	2.31(18)
V824 Cas	0.26	10.456(1)	0.124(1)	0.229(7)	0.080(10)	0.033(9)	4.695(8)	2.829(41)	5.617(86)	1.88(26)
BP Cas	0.62	10.126(1)	0.264(1)	0.370(4)	0.136(4)	0.065(7)	1.375(4)	3.321(15)	5.791(31)	3.557(51)
CH Cas	0.85	10.044(2)	0.359(3)	0.354(12)	0.206(5)	0.123(9)	0.134(9)	2.996(23)	5.449(69)	2.074(85)

Table 8. Amplitude and Fourier coefficients of the sample Cepheids in I filter.

Star	A [mag]	A_0 [mag]	A_1 [mag]	R_{21}	R_{31}	R_{41}	Φ_1 [rad]	Φ_{21} [rad]	Φ_{31} [rad]	Φ_{41} [rad]
DF Cas	0.41	9.631(1)	0.166(1)	0.409(5)	0.169(6)	0.086(8)	0.530(7)	3.040(21)	6.195(40)	3.011(61)
V395 Cas	0.33	9.388(1)	0.147(1)	0.339(5)	0.104(6)	0.048(5)	3.311(7)	2.858(25)	0.101(65)	2.84(15)
UZ Cas	0.51	10.117(1)	0.211(2)	0.378(8)	0.175(10)	0.092(8)	2.029(7)	3.035(33)	5.943(53)	2.955(90)
CG Cas	0.56	9.850(3)	0.223(2)	0.421(11)	0.178(10)	0.057(8)	0.742(20)	2.974(53)	6.122(84)	3.70(23)
CF Cas	0.34	9.718(1)	0.155(1)	0.281(6)	0.127(6)	0.044(5)	1.886(6)	3.284(21)	0.706(44)	2.61(13)
DW Cas	0.38	9.514(1)	0.162(2)	0.364(16)	0.128(20)	0.044(17)	0.887(17)	3.174(63)	6.23(0.11)	2.94(26)
V824 Cas	0.21	9.554(1)	0.097(1)	0.262(6)	0.036(7)	0.037(8)	4.607(6)	3.006(29)	5.99(15)	2.69(15)
BP Cas	0.5	9.156(1)	0.214(1)	0.368(5)	0.144(5)	0.043(7)	1.477(5)	3.481(17)	6.101(33)	4.19(11)
CH Cas	0.7	8.945(2)	0.292(4)	0.362(16)	0.206(7)	0.117(12)	0.032(11)	3.176(28)	5.784(92)	2.53(12)